Published in final edited form as:

J Immunol. 2015 November 15; 195(10): 4810–4821. doi:10.4049/jimmunol.1500414.

NK Cell Proliferation Induced by IL-15 Transpresentation Is Negatively Regulated by Inhibitory Receptors

Olga M. Anton[*,1], **Susina Vielkind**[*,1], **Mary E. Peterson**[*], **Yutaka Tagaya**[†], and **Eric O. Long**[*]

[*]Laboratory of Immunogenetics, National Institute of Allergy and Infectious Diseases, National Institutes of Health, Rockville, MD 20852

[†]Division of Basic Science and Vaccine Research, Institute of Human Virology, University of Maryland School of Medicine, Baltimore, MD 21201

Abstract

IL-15 bound to the IL-15 receptor α chain (IL-15Rα) is presented in *trans* to cells bearing the IL-2 receptor β and γ_c chains. As IL-15 transpresentation occurs in the context of cell-to-cell contacts, it has the potential for regulation by and of other receptor–ligand interactions. In this study, human NK cells were tested for the sensitivity of IL-15 transpresentation to inhibitory receptors. Human cells expressing HLA class I ligands for inhibitory receptors KIR2DL1, KIR2DL2/3, or CD94-NKG2A were transfected with IL-15Rα. Proliferation of primary NK cells in response to transpresented IL-15 was reduced by engagement of either KIR2DL1 or KIR2DL2/3 by cognate HLA-C ligands. Inhibitory KIR–HLA-C interactions did not reduce the proliferation induced by soluble IL-15. Therefore, transpresentation of IL-15 is subject to down-regulation by MHC class I-specific inhibitory receptors. Similarly, proliferation of the $NKG2A^+$ cell line NKL induced by IL-15 transpresentation was inhibited by HLA-E. Co-engagement of inhibitory receptors, either KIR2DL1 or CD94-NKG2A, did not inhibit phosphorylation of Stat5 but inhibited selectively phosphorylation of Akt and S6 ribosomal protein. IL-15Rα was not excluded from, but was evenly distributed across inhibitory synapses. These findings demonstrate a novel mechanism to attenuate IL-15 dependent NK cell proliferation and suggest that inhibitory NK cell receptors contribute to NK cell homeostasis.

Keywords

IL-15; Inhibitory receptor; Interleukin; NK cells; Proliferation

Address correspondence and reprint requests to Dr. Eric O. Long, Laboratory of Immunogenetics, national Institute of Allergy and Infectious Diseases, National Institutes of Health, 12441 Parklawn Drive, Rockville, MD 20852. eLong@nih.gov.

[1]These authors made equal contributions

The online version of this article contains supplemental material.

Disclosures

The authors have no financial conflicts of interest.

Introduction

IL-15 is essential for NK cell survival, differentiation, and proliferation (1). The IL-15 receptor (IL-15R) consists of the three subunits α, β and γ_c. Whereas the α chain (IL-15Rα) is unique to the IL-15R, the β chain (IL-2Rβ) is shared with the IL-2 receptor and the common γ (γ_c) chain is shared with members of the cytokine receptor family, which includes IL-2R, IL-4R, IL-7R, IL-9R, IL-15R, and IL-21R (2). NK cells do not develop in mice lacking any one of the components of IL-15 and its receptor, such as IL-15$^{-/-}$, IL-15Rα$^{-/-}$, IL-2/15Rβ$^{-/-}$, and $\gamma_c^{-/-}$ mice (3–8), nor in mice defective in IL-15 signaling, including Jak3$^{-/-}$ and Stat5a/b$^{-/-}$ mice (9–11), thus highlighting the essential and specific role of IL-15.

Despite their shared use of IL-2Rβ and γ_c to transmit signals, IL-2 and IL-15 stimulate cells by different mechanisms. IL-15 is bound with high affinity (K_d 10^{-11} M) to IL-15Rα, which is expressed on cells that present IL-15 in *trans* to the IL-2Rβγ_c subunits expressed on lymphocytes (12). The IL-15–IL-15Rα complex undergoes multiple rounds of endocytosis and recycling (12). At high concentrations in vitro, soluble IL-15 can signal directly via the intermediate affinity (K_d 10^{-9} M) IL-2Rβγ_c complex, which is expressed on NK cells (12, 13). IL-15Rα expression on NK cells is not required for their survival (13). IL-15 and IL-15Rα must be coordinately expressed by the same cells to support NK cell development *in vivo* (14). Physiological sources of IL-15 are monocytes (15), stromal cells (16), and dendritic cells (DC). Physiological niches for interaction of NK cells with IL-15 transpresenting cells are the bone marrow and secondary lymphoid organs where NK cells reside and receive stimulatory signals required for their differentiation and activation (17, 18). DC have an essential role in priming and stimulating NK cells (19–23).

Activated NK cells are potent cytotoxic effectors through release of cytolytic proteins such as perforin and granzymes, and have immunoregulatory activity through secretion of cytokines and chemokines (e.g. TNF-α, IFN-γ, MIP-1α) (18, 24). NK cell responses to target cells are under control of inhibitory receptors, which recognize primarily MHC class I molecules (25, 26). The human MHC class I-specific inhibitory receptors include members of the killer cell Ig-like receptor (KIR) family and the CD94-NKG2A lectin-like heterodimer, both of which carry immunoreceptor tyrosine-based inhibition motifs (ITIM) in their cytoplasmic tail, which mediate inhibition through recruitment of the tyrosine phosphatase SHP-1 (26, 27). A second component of the inhibitory pathway relies on phosphorylation of the small adaptor Crk and its dissociation from cytoskeletal scaffold proteins (28, 29).

Presentation of IL-15 in *trans* by cells that express IL-15Rα, rather than direct binding of soluble IL-15 to cells co-expressing the three chains of IL-15R, must have evolved to fulfill important biological functions. It may ensure that expansion and activation of NK cells occurs only after interaction with other cell types at specific sites. For instance, bone marrow stromal cells provide signals for development and survival, and dendritic cells in lymph nodes provide priming signals (30). In addition, the very high affinity of IL-15 for IL-15Rα, and the ability of IL-15Rα–IL-15 complexes to recycle to the cell surface may result in sustained activation of T cells and NK cells (12, 31). A fundamental difference

between activation by a soluble and a transpresented cytokine is that transpresentation can be subjected to regulation by other interactions between the presenting and the responding cells. It is not known whether IL-15 transpresentation by IL-15Rα to IL-2Rβγ_c chains in NK cells is a potential target of inhibitory receptor signaling. Here we have addressed this question using human NK cells (primary NK cells and an NK cell line) and cells engineered to express IL-15Rα in combination with HLA class I ligands for inhibitory receptors. Our results have shown that IL-15 transpresentation is negatively regulated by co-engagement of inhibitory receptors.

Materials and Methods

Cells and Antibodies

Human NK cells were isolated from peripheral blood mononuclear cells by depletion of non-NK cells using an NK cell isolation kit (Miltenyi Biotech, Auburn, CA). Human blood samples from anonymized healthy donors was drawn for research purposes at the NIH Blood Bank under an NIH IRB approved protocol with informed consent. NK cell purity was assessed by flow cytometry; cells were ≥98% $CD3^-CD56^+NKp46^+$. In some experiments, NKG2C positive cells were depleted by negative selection following a described protocol (29). The human NK cell line NKL (a gift of M. Robertson, Indiana University Medical Center, Indianapolis, IN) (32) was cultured in RPMI supplemented with 10% fetal bovine serum (FBS), and 100 U/ml rIL-2. NKL-2DL1 cells were generated by retroviral transduction. For that purpose, KIR2DL1 cDNA was cloned into the retroviral vector PCDH-EF1-MCS-T2A-Puro, by using XbaI and NotI restriction enzymes, and cells were selected using puromycin (0.3 μg/ml). Prior to IL-15 stimulation experiments, NKL cells were rested in RPMI with 10% FBS in the absence of IL-2 for 36 h, and in the absence of FBS during the last 12 h. 721.221 is human B lymphoblastoid cell line mutagenized and selected for the loss of all HLA-A, HLA-B, and HLA-C genes (33). 721.221 cells expressing HLA-Cw3 (221–Cw3), HLA-Cw4 (221–Cw4), and HLA-Cw15 (221–Cw15) were generated using a retroviral transduction method with G418 selection (500 μg/ml), as described (34). 221–IL-15Rα, 221–Cw3–IL-15Rα, 221–Cw4–IL-15Rα and 221–Cw15–IL-15Rα were generated by transduction with a human IL-15Rα cDNA in the retroviral vector pBabe (35) carrying blasticidin selection (3.2 μg/ml). 721.221 cells expressing HLA-E (221-AEH cells, a gift from D. Geraghty, Fred Hutchinson Cancer Research Center, Seattle) (36), thereafter referred to as 221–E, were transfected with IL-15Rα in the same retroviral vector but using a VSV-G pseudotype retroviral transduction system (37) to generate 221–E–IL-15Rα cells using blasticidin selection (3.4 μg/ml). 221–IL-15Rα-Cherry cells were generated by transfection with a human IL-15Rα cDNA cloned into the pmCherry-N1 vector, using XhoI and BamH1 restriction enzymes, and selection in 0.5 mg/ml G418. Transfected 721.221 cells were maintained in Iscove's Modified Dulbecco's Medium (IMDM) supplemented with 10% FBS and L-glutamine.

The following antibodies were used: CD158a (EB6) to detect KIR2DL1 and KIR2DS1; CD158b (GL183) to detect KIR2DL2, KIR2DL3, and KIR2DS2; CD159a (Z199) to detect NKG2A and anti-IL15 (clone 34593) all from Beckman Coulter. The cyt42/43 polyclonal antiserum specific for the long cytoplasmic tail of KIR2DL1 and KIR2DL2 was produced in

rabbits after immunization with peptide AESRSKVVSCP conjugated to KLH (38). The cyt6 antiserum specific for the cytoplasmic tail of KIR2DL3 was produced the same way with peptide VYTELPNAES (27). Anti-NKG2C (134522) was from R&D, mAb to CD107a (H4A3), CD132 (TUGh4) to detect γ_c, CD122 (Mik-β3) to detect IL-2Rβ were from Pharmingen. Anti-phospho-Ser235Ser236-S6 (2F9) coupled to Alexa 488 and anti-phospho-Ser473-Akt were from Cell Signaling and anti-HLA-E (MEM-E/07) was from Exbio (Prague, Czech Republic). Anti-phospho-Tyr694-Stat5 coupled to APC was from BD Biosciences. HLA-C was detected using F4/326 (IgG2a), a gift from S.Y. Yang (Memorial Sloan-Kettering Cancer Center, New York). Anti-human IL-15Rα mAb has been described (12). Secondary anti-rabbit and anti-mouse antibodies coupled to Alexa 488 were from Molecular Probes and secondary anti-mouse antibody coupled to PE was from Jackson Laboratories.

IL-15 Loading for Transpresentation by IL-15Rα Transfected Cells

For all transpresentation experiments, 721.221 cells expressing IL-15Rα were resuspended in phosphate buffered saline (PBS) and 1% fetal bovine serum (FBS), incubated for 20 min at 37°C in 5% CO_2 with IL-15 at a final concentration of 50 nM, unless stated otherwise, and washed 3 times in complete medium.

Proliferation and Survival Assay

For assays using 221–IL-15Rα cells, both resting human NK cells and rested NKL cells were adjusted to 5×10^6 cells/ml in IMDM, 0.1% bovine serum albumin (BSA) and labeled with Carboxyfluorescein succinimidyl ester (CFSE) (Molecular Probes) at 2.5 μM for 5 min at 37°C, followed by two washes in IMDM supplemented with 10% human serum (HS) (Valley Biomedical). NK cells were adjusted to 1×10^6 cells/ml in IMDM, 10% HS and mixed at a 1:1 ratio with 221–IL-15Rα cells, that had been irradiated (4500 rads) and preloaded with IL-15. Proliferation of NK cells was assayed after 3 to 5 days by flow cytometry analysis of CFSE dilution in combination with antibodies for KIR2DL1, KIR2DL2/3, NKG2A and NKG2C. Propidium Iodide (PI) incorporation was used to detect dead cells and exclude them from the analysis. Some of the flow cytometry data was expressed as division indices using FlowJo analysis software. The division index incorporates the number of divisions in the dividing cell population as well as the fraction of cells in the starting population that have divided. Proliferation of NK cells was assayed at days 3 or 5, as indicated, by flow cytometry analysis of CFSE dilution. For cell survival assays, NKL cells were rested for 24 h in medium with no FCS or IL-2, labeled with CFSE and mixed with irradiated cells expressing the IL-15Rα chain that had been preloaded with low doses of IL-15 (0.5 and 0.05 nM, as indicated). $CFSE^+$ cells were gated in live cells (PI negative) and cell counts were obtained by flow cytometry every 24 h.

Intracellular Flow Cytometry

For phospho-Stat5, phospho-S6 and phospho-Akt assays, 3×10^6 NKL cells or 5×10^6 primary NK cells were resuspended in IMDM, 10% human serum, and were either left unstimulated or stimulated for 1h, in the case of phospho-Stat5 and phospho-S6 detection, or 30 minutes, to detect phospho-Akt, with 50 nM soluble IL-15 as control. For stimulation by transpresentation, 5×10^5 NK cells were mixed for 1h, in the case of phospho-Stat5 and

phospho-S6 detection, or 30 minutes, to detect phospho-Akt, with 5×10^5 irradiated and IL-15-preloaded 221 cells expressing IL-15Rα in 1 ml IMDM, 10% HS. Following stimulation, cells were centrifuged for 2 min at 1500 rpm, washed once with PBS, and stained with a PE-conjugated anti-NKG2A antibody for 30 min at 4°C and then fixed for 10 min at room temperature using the BD Phosphoflow Lysis/Fix buffer (BD biosciencies). The cells were washed once in PBS and permeabilized using the BD Phosphoflow Perm buffer III (BD biosciencies) at −20°C for 30 min. Cells were washed twice in PBS, 1% FBS and stained with APC-conjugated anti-phospho-Stat5 and Alexa488-conjugated anti-phospho-S6 for 30 min at 4°C. For detection of phospho-Akt, a primary anti phospho-Akt Ab and a secondary Ab coupled to Alexa 488 were used. Gating on NKL cells was performed with a PE-conjugated anti-NKG2A Ab. Primary NK cells were gated using anti Abs to NKG2A and CD56. Cells were then washed once in PBS, 1% FBS and resuspended for flow cytometry analysis.

Immunofluorescence analysis

NKL cells were mixed with an equal number of 221 cells for 20 min at 37°C and added onto poly-L-lysine coated coverslips. Cells were fixed in 10% Formalin solution (Sigma-Aldrich) for 20 min, rinsed, and treated with 10 mM glycine in PBS for 5 min to quench the aldehyde groups. Cells were then washed, permeabilized with 0.2% Triton X-100 in PBS at 4°C for 5 min, rinsed, incubated with 3% (w/v) BSA for 15 min, and incubated with the primary antibody. After 1 h at room temperature, cells were washed and incubated with the appropriate fluorescent secondary Ab. Immunofluorescence images were obtained using a LSM 780 Confocal Laser microscope (Carl Zeiss, Oberkochen, Germany) equipped with a 63× objective (1.4 numerical aperture oil immersion objective; Carl Zeiss). Images were acquired using the Zen software (Carl Zeiss) and analyzed using Image J (National Institutes of Health; http://rsb.info.nih.gov/ij). The fluorescence intensity of IL-15Rα-Cherry was represented by a pseudocolored scale (0–256). To analyze the enrichment of molecules at the contact between 221 and NK cells, we focused on single NK–221 conjugates. Fluorescence intensity was measured along the site of contact and compared with the intensity of signal at the opposite pole of the cell. The distribution of molecules along the width of the site of contact, was determined in three equal segments by measuring the fluoresce intensity, using Image J. The fluorescence intensity at the two distal segments was averaged and compared with the fluorescence intensity at the center.

Results

NK cell proliferation induced by IL-15 transpresentation is negatively regulated by coengagement of inhibitory KIR

To test whether signals induced by IL-15 transpresentation are sensitive to inhibitory receptors expressed on NK cells, the HLA class I-negative human cell line 721.221 was transfected with IL-15Rα either alone (221–IL-15Rα) or in combination with HLA-Cw3 (221–Cw3–IL-15Rα) or HLA-Cw4 (221–Cw4–IL-15Rα) (Figure 1A, and Figure S1A-B). HLA-Cw3 is a ligand for inhibitory KIR2DL2 and KIR2DL3, whereas HLA-Cw4 is a ligand for inhibitory KIR2DL1. 721.221 cells expressing IL-15Rα were irradiated prior to loading with soluble IL-15 and stimulation of NK cell proliferation. 221–IL-15Rα cells that

were preloaded with IL-15 induced proliferation of resting human NK cells, as detected by CFSE dilution after 5 days (Figure 1A). No proliferation was observed when resting NK cells were incubated with 221–IL-15Rα cells that had not been loaded with IL-15. Therefore, 721.221 cells transfected with IL-15Rα provide a suitable system to evaluate the sensitivity of IL-15 transpresentation to signaling by inhibitory receptors.

NK cells express several MHC class I-specific inhibitory receptors, which are distributed almost randomly among individual NK cells. Therefore, to study inhibition of primary, resting NK cells it is necessary to identify NK cells that express a given receptor of known specificity by flow cytometry. Furthermore, the KIR family includes receptors with long cytoplasmic tails, which are inhibitory, and receptors with short cytoplasmic tails, which are activating (39, 40). The mAb GL183 binds to inhibitory KIR2DL2 and KIR2DL3 and to the activating KIR2DS2. Likewise, mAb EB6 binds to inhibitory KIR2DL1 and activating KIR2DS1. Therefore, it was necessary to identify donors who lack NK cells that express KIR2DS1 or KIR2DS2 in the absence of inhibitory receptors, using polyclonal antisera specific for the long cytoplasmic tails of inhibitory KIR (Figure 1B). In the example shown, $EB6^+$ cells were also positively stained with polyclonal antiserum cyt42-43 raised against the C-terminal amino acids of the cytoplasmic tail of inhibitory KIR2DL1 and KIR2DL2 (cyt42-43). Therefore this donor had very fey or no NK cells that express KIR2DS1 in the absence of KIR2DL1. Among $GL183^+$ cells, some were positively stained with cyt42-43, indicating KIR2DL2 expression. $GL183^+$ cells not reactive with cyt42-43 include $KIR2DL3^+$ and $KIR2DS2^+$ cells. To distinguish between the two, cells were also stained with polyclonal antiserum cyt6, which reacts with the cytoplasmic tail of KIR2DL3, together with the antiserum cyt42-43 (Figure 1B). The result showed that all the $GL183^+$ cells reacted with antisera specific for the inhibitory tails. Therefore, primary NK cells from this donor did not include NK cells that express KIR2DS1 or KIR2DS2 in the absence of inhibitory KIR2DL1 or KIR2DL2/3. Throughout our study, all donors were screened as shown here. NK cells from donors that expressed KIR2DS1 or KIR2DS2 on NK cells devoid of inhibitory receptors KIR2DL1, KIR2DL2 or KIR2DL3 were not used.

To test the impact of inhibitory KIR coengagement on proliferation induced by IL-15 transpresentation, 221–Cw3–IL-15Rα and 221–Cw4–IL-15Rα cells were preincubated with soluble IL-15 and receptor bound IL-15 was monitored by flow cytometry (Figure 1C). NK cells were mixed with equal numbers of transpresenting 221–Cw3–IL-15Rα or 221–Cw4–IL-15Rα cells and the dilution of CFSE was monitored by flow-cytometry after 5 days. The proliferation of $KIR2DL2/3^+$ cells in response to 221–Cw3–IL-15Rα cells was lower than the proliferation of $KIR2DL1^+$ cells (Figure 1D). Conversely, fewer $KIR2DL1^+$ cells underwent cell division in response to 221–Cw4–IL-15Rα cells than $KIR2DL2/3^+$ cells (Figure 1D). $KIR2DL1^+$ and $KIR2DL2/3^+$ cells expressed equal amounts of the intermediate affinity receptor for IL-15 (IL-2Rβ and γ_c chains) and did not express IL-15Rα (Figure S2). The negative impact of KIR engagement on proliferation was typically more pronounced in the commitment to divide than the number of divisions by committed cells. There was variability among individual donors in the repertoire of KIRs expressed by NK cells and in the capacity of NK cell subsets to proliferate. Nevertheless, we consistently observed a fraction of NK cells that did not undergo cell division in response to IL-15 transpresentation in the context of inhibitory HLA-C ligand. Results from three representative donors, which

illustrate the variability among donors, are shown in Figure 1E. These experiments were internally controlled given that KIR2DL1$^+$ and KIR2DL2/3$^+$ cells were compared within the same sample, during interaction with the same transpresenting cells. We conclude that proliferation of freshly isolated, primary NK cells induced by IL-15 transpresentation is under negative regulation by inhibitory KIR.

We then asked whether KIR-mediated inhibition would also block proliferation induced by soluble IL-15. Primary NK cells from a donor that did not include NK cells expressing KIR2DS2 in the absence of inhibitory KIR2DL1 or KIR2DL2/3 (Figure 2A) were mixed with 221–Cw3–IL-15Rα cells that had been loaded with IL-15 (Figure 2B). The total NK cell population proliferated strongly (Figure 2C). Whereas most of the cells gated for KIR2DL1$^+$ and negative for KIR2DL2/3, NKG2A and NKG2C proliferated well, a large fraction of cells gated for KIR2DL2/3$^+$ and negative for KIR2DL1, NKG2A and NKG2C did not undergo cell division (Figure 2C), in agreement with previous experiments (Figure 1). To test for inhibition of proliferation induced by soluble IL-15, the same primary NK cell population was mixed in the presence of 50 nM soluble IL-15 with 721.221 cells that were not transfected with IL-15Rα (221) and 721.221 cells transfected with HLA-Cw3 (221–Cw3). There was no difference in the CFSE profiles of the KIR2DL1$^+$ and KIR2DL2/3$^+$ subsets, gated as in Figure 2C, in response to soluble IL-15, even in the presence of target cells that express a ligand for inhibitory receptors KIR2DL2 and KIR2DL3 (Figure 2D). In summary, our results showed that inhibition of NK cell proliferation by inhibitory KIR applies to stimulation by transpresented IL-15, but not soluble IL-15.

NK cell proliferation induced by IL-15 transpresentation is inhibited by co-engagement of CD94-NKG2A

To test whether KIR-mediated inhibition of IL-15 transpresentation was a property shared with other inhibitory receptors, we monitored proliferation induced by IL-15 transpresentation during co-engagement of inhibitory receptor CD94-NKG2A, which binds HLA-E. Primary NK cells were not suitable for these experiments because NKG2A-negative NK cells cannot be depleted and, furthermore, acquired NKG2A expression in culture during the time required to monitor proliferation. Therefore, we chose the NK cell line NKL, which expresses a functional CD94-NKG2A receptor, and requires IL-2 or IL-15 for its proliferation. NKL cells were rested in the absence of soluble IL-2 or IL-15 for 36 hours prior to experiments, in order to measure their proliferation induced in response to specific stimuli. To test for inhibition of IL-15 transpresentation by CD94-NKG2A, 721.221 cells transfected with HLA-E (221–E) were super-transfected with IL-15Rα (221–E–IL-15Rα) (Figure S1C). IL-15 loading on 221–IL-15Rα and 221–E–IL-15Rα was monitored by flow cytometry (Figure 3A). NKL cells were labeled with CFSE and mixed with an equal number of 221–IL-15Rα or 221–E–IL-15Rα that had been preloaded or not with IL-15. Cell proliferation was evaluated after 3 days. NKL cells were gated by size and expression of NKG2A. Proliferation was stimulated by soluble IL-15 alone and by IL-15 transpresentation by 221–IL-15Rα cells (Figure 3B). In contrast, 221–E–IL-15Rα cells preloaded with IL-15 did not stimulate proliferation of NKL cells (Figure 3B). The viability of NKL cells remained high during incubation with 221–IL-15Rα and 221–E–IL-15Rα cells preloaded with IL-15 (Figure 3C). Over multiple experiments, NKL proliferation was

minimal during IL-15 transpresentation by cells expressing HLA-E (Figure 3D). However, this experimental system did not exclude the possibility that IL-15 bound to IL-15Rα expressed on 221–E cells somehow failed to be transpresented to the IL-2Rβγc complex on NK cells. This point will be addressed later.

As IL-15 is necessary for NK cell survival, it is possible that the lack of proliferation during inhibition of IL-15 transpresentation was due, at least in part, to cell death. We therefore examined the survival of NKL cells during IL-15 transpresentation by 221–IL-15Rα and 221–E–IL-15Rα cells. We first selected conditions under which NKL cells survived without proliferating. Preloading of 221–IL-15Rα cells in 0.5 and 0.05 nM was sufficient to promote survival of NKL cells during transpresentation (Figure S3A). 221–IL-15Rα and 221–E–IL-15Rα cells preloaded at these two concentrations were mixed with NKL cells, and NKL cell survival was determined by the lack of PI incorporation at different days (Figure S3B). Cell viability dropped at day 4 and 5 after mixing with 221–IL-15Rα and 221–E–IL-15Rα cells that had not been preloaded with IL-15. In contrast, NKL cells incubated with IL-15 preloaded 221–IL-15Rα showed better survival at day 4 and 5 (Figure S3B). Furthermore, there was equally good survival of NKL cells incubated with IL-15-preloaded 221–E–IL-15Rα cells. We concluded that, in contrast to the inhibition of proliferation during transpresentation at inhibitory synapses, NK cell survival was not affected.

S6 phosphorylation, but not Stat5 phosphorylation induced by IL-15 transpresentation is inhibited by co-engagement of CD94-NKG2A

IL-2 or IL-15 binding to IL-2Rβγc activates two signaling pathways: the JAK3-Stat5 pathway, that leads to a transcriptional response, and a phosphoinositide 3-kinase (PI-3K)–Akt–mammalian target of rapamycin (mTOR)C1 pathway required for proliferation (41). The signaling pathway for proliferation involves phosphorylation of the ribosomal protein S6 by the p70-S6 kinase. Since NKG2A engagement on NK cells did reduce the proliferation induced by IL-15 transpresentation, we tested the sensitivity of the two signaling pathways to inhibition. Addition of soluble IL-2 (100 U/ml) or IL-15 (50 nM) to NKL cells induced phosphorylation of both Stat5 and S6, as monitored by flow cytometry (Figure 4A). NKL cells were mixed with 221–IL-15Rα cells that had been preloaded or not with IL-15, and incubated for 1 hour before fixation and staining with specific anti phospho-antibodies. IL-15 transpresentation induced phosphorylation of both Stat5 and S6 (Figure 4B). 221–IL-15Rα cells that had not been loaded with IL-15 induced S6 phosphorylation in a large fraction of NKL cells (Figure 4B). However, the S6 phosphorylation induced by 221 cells in the absence of IL-15 transpresentation was not accompanied by cell division (Figure 3B, 3D). To test the sensitivity of each of these two pathways to inhibition by CD94-NKG2A, NKL cells were mixed with 221–E–IL-15Rα. 221–E–IL-15Rα cells preloaded with IL-15 induced Stat5 phosphorylation in NKL cells, which was as strong as that induced by 221–IL-15Rα cells (Figure 4C). In contrast, phosphorylation of S6 induced by 221–E–IL-15Rα cells preloaded with IL-15 was reduced in a large fraction of NKL cells, when compared to 221–IL-15Rα cells (Figure 4C). The S6 phosphorylation induced by 221–IL-15Rα cells that were not preloaded with IL-15 (Figure 4B) was also inhibited upon NKG2A engagement by HLA-E (Figure 4C). Therefore, the inhibition of S6 phosphorylation observed in NKL cells incubated with IL-15-loaded 221–E–IL-15Rα cells

may be due to the combined inhibition of IL-15-dependent and IL-15-independent S6 phosphorylation. To confirm that inhibition was due to CD94-NKG2A, we performed the same experiment in the presence of the blocking anti-NKG2A antibody Z199 or the IgG2b isotype control MOPC41 (Figure 4C). Strong phosphorylation of S6 in most NKL cells, comparable to that observed after stimulation with 221–IL-15Rα cells preloaded with IL-15, was restored in the presence of Z199 (Figure 4C). Therefore, we conclude that the inhibition of S6 phosphorylation during IL-15 transpresentation was due to the engagement of the inihibitory receptor NKG2A on NKL.

These results (Figure 4) showed also that 221–E–IL-15Rα cells were capable of transpresenting IL-15, and that the lack of proliferation (Figure 3) was due to inhibition by HLA-E rather than an inability of 221–E–IL-15Rα cells to transpresent IL-15. Quantitation of Stat5 and ribosomal protein S6 phosphorylation observed in several experiments confirmed that engagement of inhibitory receptor CD94-NKG2A by its ligand HLA-E on transpresenting cells inhibited the phosphorylation of S6 but not Stat5 (Figure 4D). These results are consistent with a role of the JAK-Stat pathway in providing survival signals (42, 43) and with our observation that NK cell survival induced by low-dose IL-15 transpresentation was not affected by NKG2A co-engagement (Figure S3).

Akt phosphorylation induced by IL-15 transpresentation is inhibited by co-engagement of CD94-NKG2A

The interpretation of the previous experiment was complicated by two factors. First, incubation of NKL cells with 221–IL-15Rα cells that had not been preloaded with IL-15 resulted in S6 phosphorylation in a large fraction of NKL cells. Second, co-engagement of CD94-NKG2A with HLA-E did not completely block S6 phosphorylation. As NKL proliferation was not induced by 221–IL-15Rα cells that had not been preloaded with IL-15, and proliferation induced by preloaded 221–IL-15Rα cells was inhibited by HLA-E expression (Figure 3), S6 phosphorylation in NKL cells was not a good indicator of cell proliferation. Therefore, we chose to examine another component of the signaling pathway for proliferation that would be proximal to p70-S6 kinase. The Ser/Thr kinase Akt is an important player in the PI-3K–mTORC1–p70S6 kinase pathway, and its activity requires PI-3K dependent phosphorylation at Ser473. We examined Akt phosphorylation with an antibody for p-S473 Akt by flow cytometry. Detection of p-S473 Akt in NKL cells incubated with 221–IL-15Rα cells required preloading with IL-15 (Figure 5A). Furthermore, preloading of 221–E–IL-15Rα cells with IL-15 did not induce p-S473 Akt in NKL cells (Figure 5B). To test whether Akt phosphorylation was inhibited by CD94-NKG2A co-engagement with IL-2Rβ/γ_c, or whether 221–E–IL-15Rα cells preloaded with IL-15 were not capable of inducing Akt phosphorylation, we performed a blocking experiment with an antibody to NKG2A. In the presence of the blocking antibody Z199 Akt phosphorylation induced by 221–E–IL-15Rα cells preloaded with IL-15 was as high as that induced by IL-15-preloaded 221–IL-15Rα cells (Figure 5B, right panel). Quantitative analysis of several experiments confirmed that engagement of inhibitory receptor CD94-NKG2A by its ligand HLA-E on cells that transpresented IL-15 inhibited Akt phosphorylation (Figure 5C). In these experiments, Akt phosphorylation at S473 correlated directly with proliferation, as it was not induced by 221 cells in the absence of IL-15

transpresentation and was fully inhibited by CD94-NKG2A binding to HLA-E on transpresenting cells.

S6 phosphorylation, but not Stat5 phosphorylation induced by IL-15 transpresentation is inhibited by co-engagement of inhibitory KIR2DL1

To test if engagement of inhibitory KIR2DL1 resulted also in selective inhibition of S6 phosphorylation, we used NKL cells stably transfected with KIR2DL1 (NKL-2DL1). To validate NKL-2DL1 cells for these experiments, we first performed proliferation experiments using IL-15-preloaded 221–IL-15Rα or 221–Cw15–IL-15Rα cells (Figure S4A). NKL-2DL1 cells underwent cell division in response to soluble IL-15 and to preloaded 221–IL-15Rα cells, but not preloaded 221–Cw15–IL-15Rα cells (Figure S4B and S4D). The inhibition of proliferation by KIR2DL1 co-engagement was not accompanied by increased cell death (Figure S4C). We then proceeded to test Stat5 and S6 phosphorylation in NKL-2DL1 cells. Addition of soluble IL-2 (100 U/ml) or IL-15 (50 nM) induced phosphorylation of both Stat5 and S6, as monitored by flow cytometry (Figure 6A). IL-15 transpresentation by 221–IL-15Rα cells induced phosphorylation of both Stat5 and S6 in most cells (Figure 6B). S6 phosphorylation in NKL-2DL1 cells after incubation with 221–IL-15Rα cells that had not been preloaded with IL-15 occurred in only a few cells (Figure 6B), in contrast to untransfected NKL cells (Figure 4). IL-15 transpresentation by 221–Cw15–IL-15Rα cells induced strong Stat5 phosphorylation but no more S6 phosphorylation than that observed after incubation with 221–Cw15–IL-15Rα cells that had not been preloaded with IL-15 (Figure 6C). Quantitation of Stat5 and ribosomal protein S6 phosphorylation observed in several experiments confirmed that engagement of inhibitory receptor KIR2DL1 by its ligand HLA-Cw15 on cells that transpresented IL-15 inhibited the phosphorylation of S6 but not Stat5 (Figure 6D).

S6 phosphorylation, but not Stat5 phosphorylation induced by IL-15 transpresentation is inhibited by co-engagement of CD94-NKG2A in primary human NK cells

We wanted to test whether the selective inhibition S6 phosphorylation, over that of Stat5, was also featured in primary NK cells. The inhibitory receptor NKG2A is expressed on a large fraction of the total NK cell population (about 60–70%), whereas the activating receptor NKG2C, which is also a ligand for HLA-E, is less common on primary NK cells (usually 5–15% in the total population). Therefore, to test inhibition by NKG2A, primary NK cells were depleted of $NKG2C^+$ cells and mixed with 221–IL-15Rα cells or 221–E–IL-15Rα cells that had been pre-loaded or not with IL-15 for 1 hour before fixation, and stained with anti phospho-Stat5 and phospho-S6 antibodies. For analysis, $CD56^+$ cells were gated into $NKG2A^-$ (left panels) and $NKG2A^+$ (right panels) cells. The extent of Stat5 and S6 phosphorylation induced by IL-15-loaded 221–IL-15Rα cells was very similar in $NKG2A^-$ and $NKG2A^+$ populations (Figure 7A, B). After mixing with IL-15-loaded 221–E–IL-15Rα cells, phosphorylation of Stat5 was similar in the two $NKG2A^-$ and $NKG2A^+$ subsets (Figure 7C), and was very similar to that observed after transpresentation by 221–IL-15Rα cells. In contrast, after mixing with IL-15-loaded 221–E–IL-15Rα cells, S6 phosphorylation was inhibited selectively in $NKG2A^+$ NK cells, as compared to $NKG2A^-$ cells (Figure 7D). The small amount of phospho-S6 induced by 221–IL-15Rα cells that had not been preloaded with IL-15 was also inhibited by HLA-E in $NKG2A^+$ NK cells (Figure

7B, D). The results of Stat5 phosphorylation and S6 phosphorylation were confirmed in several experiments (Figure 7E, F). We conclude that the selective inhibition of S6 during transpresentation of IL-15 in the context of an inhibitory synapse occurs in primary, resting human NK cells.

Polarization of IL-15Rα at synapses with NK cells

IL-15Rα expressed on dendritic cells accumulates at synapses with NK cells, concomitant with accumulation of KIR and CD94-NKG2A inhibitory receptors, integrin LFA-1, and talin on the NK cells (44). In DC, IL-15Rα is expressed as an endogenous, pre-assembled complex with IL-15. With our reconstituted cellular system we had the opportunity to examine the distribution of IL-15Rα, preloaded or not with IL-15 at NK cell synapses that were either activating or inhibitory. To avoid specificity issues with available Abs for IL-15Rα, we generated 721.221 cells stably expressing IL-15Rα fused to the fluorescent protein mCherry, either alone (221–IL-15Rα-Cherry) or in combination with HLA-E (221–E–IL-15Rα-Cherry). Expression of IL-15Rα at the surface of these two transfectants was similar (figure S1D). IL-15 loading was monitored by flow cytometry with an antibody for IL-15 (Figure 8A). Confocal microscopy with NKL cells in contact with 221–IL-15Rα-Cherry or 221–E–IL-15Rα-Cherry cells that were fixed and stained with an antibody for perforin revealed that IL-15Rα accumulated at synapses only after preloading with IL-15 (Figure 8B). As expected, perforin-containing granules were polarized towards activating synapses with 221–IL-15Rα-Cherry cells, but not inhibitory synapses with 221–E–IL-15Rα-Cherry cells (Figure 8B). Accumulation of IL-15-preloaded IL-15Rα-Cherry was quantified by the fluorescence signal and expressed as fold enrichment of receptor at the synapse area ($MFI_{(A)}$), as compared to the opposite pole of the cell ($MFI_{(B)}$) (Figure 8C). IL-15Rα-Cherry was enriched at both activating and inhibitory synapses, but its distribution was different. At activating synapses with 221–IL-15Rα-Cherry cells, IL-15Rα accumulated at the periphery of the synapse (Figure 8B, 8D). In contrast, at inhibitory synapses with 221–E–IL-15Rα-Cherry cells, IL-15Rα was distributed along the entire contact area (Figure 8B and 8D). This accumulation was quantified by the fluorescence signal and expressed as the fold enrichment of receptor at the periphery of the synapse ($MFI_{(D)}$) compared to the enrichment at the center of the synapse ($MFI_{(C)}$) (Figure 8D). These results showed that the inhibition of NKL cell proliferation and S6 phosphorylation during co-engagement of CD94-NKG2A with IL-2Rβγ_c was not due to exclusion of IL-15Rα from the synapse but to inhibition of IL-2Rβγ_c signaling.

Discussion

Transpresentation of IL-15 to NK cells by cells that express the IL-15Rα chain supports NK cell development, survival, and proliferation (12, 14). Given that transpresentation occurs in the context of a cell-to-cell interaction, it could be subject to regulation by other receptor–ligand interactions at NK cell immunological synapses with transpresenting cells. Here we have evaluated whether transpresentation of IL-15 to human NK cells is regulated by NK inhibitory receptors that bind to MHC class I on IL-15-presenting cells. The main conclusion from our study is that NK cell proliferation induced by IL-15 transpresentation is down-modulated by NK inhibitory receptors. Co-engagement of inhibitory receptor CD94-

NKG2A by HLA-E, and that of KIR2DL1 by HLA-C on cells that transpresented IL-15 resulted in diminished proliferation. Strikingly, these receptors inhibited selectively the phosphorylation of ribosomal protein S6 and phosphorylation of the Ser/Thr kinase Akt, but not phosphorylation of Stat5. These results, obtained with primary, freshly isolated NK cells and with the cell line NKL, reveal an unsuspected level of negative regulation in the response of NK cells to IL-15.

Expression of IL-15Rα on human 721.221 cells that had been transfected with different MHC class I molecules, and loading of soluble IL-15 onto 221–IL-15Rα cells for transpresentation, was used to study the sensitivity of IL-15 transpresentation to co-engagement of NK cell inhibitory receptors. 221–IL-15Rα cells not loaded with IL-15 provided a perfectly matched control for IL-15 independent NK cell proliferation. Due to the complexity of the inhibitory receptor repertoire on each NK cell and of the high genetic variability in the KIR complex, it was necessary to use assays in which NK cells were gated by flow cytometry on specific subpopulations, and to identify donors that lacked expression of activating receptors KIR2DS1 and KIR2DS2. This was achieved by staining with a combination of mAbs specific for KIR and polyclonal antisera specific for the cytoplasmic tails of inhibitory receptors (28). To correct for the possibility of differences in the intrinsic proliferative capacity of NK cell subsets and in the extent of lysis of IL-15 presenting cells by NK cells during the proliferation assay, we monitored proliferation of a single NK cell population, that was gated for expression of either KIR2DL1 (specific for HLA-Cw4) or KIR2DL2 and KIR2DL3 (both specific for HLA-Cw3), and incubated at the same time with IL-15 presenting cells expressing either HLA-Cw3 or HLA-Cw4. Such internally controlled experiments showed that co-engagement of an inhibitory KIR with IL-2Rβγ$_c$ during IL-15 transpresentation resulted in a diminished proliferative response. Direct comparison of KIR2DL1$^+$ and KIR2DL2/3$^+$ NK cells in the same culture, incubated with transpresenting cells expressing a ligand for KIR2DL1 or KIR2DL2/3 in parallel, was essential, as the proliferative capacity of NK cells varied among individual donors and in response to different transfected 721.221 cells. No inhibition was observed when NK cells, mixed with 721.221 cells expressing HLA-C, were stimulated by soluble IL-15, consistent with the fact that inhibitory receptors block activation signals locally, in the context of inhibitory immunological synapses (45). The main outcome of inhibition of transpresentation was a reduced number of NK cells that committed to proliferate, rather than a reduced number of cell divisions, suggesting that inhibition raised the signaling threshold for entry into the cell cycle.

Primary NK cells were not well suited to examine the regulation of transpresentation by CD94-NKG2A because NKG2A-negative primary NK cells acquired NKG2A expression after a few days in culture. To circumvent this problem, we used an NK cell line, NKL, that expresses CD94-NKG2A and depends on exogenous IL-2 or IL-15 for its proliferation. Prior to IL-15 transpresentation experiments, NKL cells had to be rested in the absence of IL-2. NKL cell proliferation induced by transpresentation of IL-15 was inhibited by co-engagement of CD94-NKG2A by HLA-E. This result indicated that IL-15 induced proliferation is modulated by the inhibitory receptor NKG2A. The inhibition of NKL proliferation by NKG2A was almost complete, in contrast to the down-modulation of primary NK cell proliferation by KIR2DL1 and KIR2DL2/3. This distinction is most likely

due to a difference between NKL and primary NK cells, rather than NKG2A and KIR, as proliferation of NKL cells transfected with KIR2DL1 was completely blocked by KIR2DL1 co-engagement with IL-2Rβγ$_c$ during IL-15 transpresentation. The modulation, rather than shut-down, of primary NK cell proliferation by inhibitory receptors is more compatible with the physiological situation where NK cells have to proliferate in response to MHC-I$^+$ transpresenting cells.

Previous studies have imaged the interaction of primary NK cells with myeloid-derived dendritic cells and reported the formation of a “regulatory” synapse, which shared features with NK cell inhibitory synapses while promoting NK cell survival (44). Accumulation of KIR, CD94-NKG2A, and MHC class I occurred at the regulatory synapse. Furthermore, a strong F-actin network is formed in the DC. The F-actin in the transpresenting DC may provide protection from NK cells through stabilization of MHC class I (46). In our system we had the opportunity to compare the distribution of IL-15Rα at inhibitory synapses, representative of interactions with autologous MHC-I$^+$ cells, and activating synapses, in the absence of MHC-I ligand. The accumulatation of IL-15Rα at cytotoxic immunological synapses, which are characterized by polarization of perforin-containing granules, was excluded from the center of the synapse. The center of NK cell cytotoxic immunological synapses is where degranulation occurs and where lysosomal proteins are actively retrieved by endocytosis (47). Despite this segregation of IL-15Rα away from the central area of the synapse, transpresentation of IL-15 was functional. At inhibitory synapses in our system, IL-15Rα was evenly distributed across the contact area. This result is indeed similar to its distribution at the regulatory synapse with DC (44, 46). It is also similar to the distribution of NK cell co-activation receptors 2B4 and CD2, and Fc receptor CD16, which are not excluded from inhibitory synapses formed by KIR$^+$ and CD94-NKG2A$^+$ NK cells (29, 48).

Ligand binding to the IL-2Rβγ$_c$ receptor complex activates two signaling pathways. One, leading to transcriptional activation of a large set of genes, is initiated by transphosphorylation of the JAK3 kinase, which in turn phosphorylates the transcriptional activator Stat5 (49). The other, which controls cell proliferation, is a PI3K – Akt – mTOR – p70S6-kinase pathway (50, 51). To monitor how co-engagement of CD94-NKG2A or KIR2DL1 with IL-2Rβγ$_c$ affected these two pathways, phosphorylation of Stat5 and of ribosomal protein S6 were monitored by flow cytometry. While there was no detectable inhibition of Stat5 phosphorylation, S6 phosphorylation was reduced by co-engagement of both inhibitory receptors. Blocking NKG2A with a mAb reversed the inhibition, confirming that it was mediated by CD94-NKG2A binding to HLA-E. Phosphorylation of Akt, an effector upstream of p70S6 kinase, was also inhibited by co-engagement of CD94-NKG2A. These results showed a clear and selective down-modulation by NK inhibitory receptors of the PI3K – Akt – mTOR – p70S6-kinase pathway induced by IL-15 transpresentation.

Negative regulation of JAK2 by SHP-1 has been reported for the erythropoietin (EPO) receptor (52). However, in that system, dephosphorylation of JAK2 by SHP-1 does not prevent EPO-R signaling but acts as negative feedback to return the EPO-R to its basal, unphosphorylated, state. In contrast, inhibition by SHP-1 recruitment to ITIM-bearing receptors, which include KIR and CD94-NKG2A, acts at a proximal step and prevents actin-dependent phosphorylation of co-activation receptors for natural cytotoxicity and cytokine

secretion through binding to ligands on target cells (45). In contrast to receptors that control the cytotoxic activity of NK cells, cytokine receptors signal through heterodimerization induced by ligand binding, and not through actin-dependent clustering. We have shown a selective inhibition of Akt and S6 phosphorylation, over Stat5 phosphorylation by JAK3, during co-engagement of CD94-NKG2A or KIR2DL1 with IL-2Rβγ_c. The exact point in the pathway leading to Akt and S6 phosphorylation that is directly targeted by the inhibitory signal is unknown. JAK is not a likely target of SHP-1 given that Stat5 phosphorylation is not impaired.

In contrast to the complete block of NK cell cytotoxicity achieved by inhibitory KIR binding to MHC class I, inhibition of proliferation by KIR in primary NK cells observed here was partial. This suggests that inhibitory KIR serves as a modulator of IL-15 signals for proliferation, and that NK cell responses to IL-15 transpresentation may be turned down in circumstances where MHC class I expression is upregulated, as it is in inflammatory conditions. In addition, inhibition may serve to protect NK cells from excessive stimulation; impairment of NK cell functions was noted after prolonged stimulation with a soluble IL-15Rα–IL-15 complex (53). Our findings therefore uncover a potential new role of inhibitory receptors in the regulation of NK cell homeostasis.

Supplementary Material

Refer to Web version on PubMed Central for supplementary material.

Acknowledgments

This work was supported by the Intramural Research Program at the National Institutes of Health, National Institute of Allergy and Infectious Diseases

We thank M. Robertson for NKL cells, D. Geraghty for 721.221-AEH cells and S.Y. Yang for mAb F4/326.

Abbreviations used in this article

CFSE	Carboxyfluorescein succinimidyl ester
KIR	killer cell Ig-like receptor
mTOR	mammalian target of rapamycin
PI	Propidium iodide
PI3K	phosphoinositide 3-kinase

References

1. Caligiuri MA. Human natural killer cells. Blood. 2008; 112:461–469. [PubMed: 18650461]
2. Rochman Y, Spolski R, Leonard WJ. New insights into the regulation of T cells by gamma(c) family cytokines. Nat Rev Immunol. 2009; 9:480–490. [PubMed: 19543225]
3. DiSanto JP, Muller W, Guy-Grand D, Fischer A, Rajewsky K. Lymphoid development in mice with a targeted deletion of the interleukin 2 receptor gamma chain. Proceedings of the National Academy of Sciences of the United States of America. 1995; 92:377–381. [PubMed: 7831294]
4. Kawamura T, Koka R, Ma A, Kumar V. Differential roles for IL-15R alpha-chain in NK cell development and Ly-49 induction. Journal of immunology. 2003; 171:5085–5090.

5. Kennedy MK, Glaccum M, Brown SN, Butz EA, Viney JL, Embers M, Matsuki N, Charrier K, Sedger L, Willis CR, Brasel K, Morrissey PJ, Stocking K, Schuh JC, Joyce S, Peschon JJ. Reversible defects in natural killer and memory CD8 T cell lineages in interleukin 15-deficient mice. The Journal of experimental medicine. 2000; 191:771–780. [PubMed: 10704459]

6. Lodolce JP, Boone DL, Chai S, Swain RE, Dassopoulos T, Trettin S, Ma A. IL-15 receptor maintains lymphoid homeostasis by supporting lymphocyte homing and proliferation. Immunity. 1998; 9:669–676. [PubMed: 9846488]

7. Suzuki H, Duncan GS, Takimoto H, Mak TW. Abnormal development of intestinal intraepithelial lymphocytes and peripheral natural killer cells in mice lacking the IL-2 receptor beta chain. The Journal of experimental medicine. 1997; 185:499–505. [PubMed: 9053450]

8. Vosshenrich CA, Ranson T, Samson SI, Corcuff E, Colucci F, Rosmaraki EE, Di Santo JP. Roles for common cytokine receptor gamma-chain-dependent cytokines in the generation, differentiation, and maturation of NK cell precursors and peripheral NK cells in vivo. Journal of immunology. 2005; 174:1213–1221.

9. Nosaka T, van Deursen JM, Tripp RA, Thierfelder WE, Witthuhn BA, McMickle AP, Doherty PC, Grosveld GC, Ihle JN. Defective lymphoid development in mice lacking Jak3. Science. 1995; 270:800–802. [PubMed: 7481769]

10. Park SY, Saijo K, Takahashi T, Osawa M, Arase H, Hirayama N, Miyake K, Nakauchi H, Shirasawa T, Saito T. Developmental defects of lymphoid cells in Jak3 kinase-deficient mice. Immunity. 1995; 3:771–782. [PubMed: 8777722]

11. Imada K, Bloom ET, Nakajima H, Horvath-Arcidiacono JA, Udy GB, Davey HW, Leonard WJ. Stat5b is essential for natural killer cell-mediated proliferation and cytolytic activity. The Journal of experimental medicine. 1998; 188:2067–2074. [PubMed: 9841920]

12. Dubois S, Mariner J, Waldmann TA, Tagaya Y. IL-15Ralpha recycles and presents IL-15 In trans to neighboring cells. Immunity. 2002; 17:537–547. [PubMed: 12433361]

13. Koka R, Burkett PR, Chien M, Chai S, Chan F, Lodolce JP, Boone DL, Ma A. Interleukin (IL)-15R[alpha]-deficient natural killer cells survive in normal but not IL-15R[alpha]-deficient mice. The Journal of experimental medicine. 2003; 197:977–984. [PubMed: 12695489]

14. Burkett PR, Koka R, Chien M, Chai S, Boone DL, Ma A. Coordinate expression and trans presentation of interleukin (IL)-15Ralpha and IL-15 supports natural killer cell and memory CD8+ T cell homeostasis. The Journal of experimental medicine. 2004; 200:825–834. [PubMed: 15452177]

15. Doherty TM, Seder RA, Sher A. Induction and regulation of IL-15 expression in murine macrophages. Journal of immunology. 1996; 156:735–741.

16. Ogasawara K, Hida S, Azimi N, Tagaya Y, Sato T, Yokochi-Fukuda T, Waldmann TA, Taniguchi T, Taki S. Requirement for IRF-1 in the microenvironment supporting development of natural killer cells. Nature. 1998; 391:700–703. [PubMed: 9490414]

17. Ma A, Koka R, Burkett P. Diverse functions of IL-2, IL-15, and IL-7 in lymphoid homeostasis. Annual review of immunology. 2006; 24:657–679.

18. Vivier E, Tomasello E, Baratin M, Walzer T, Ugolini S. Functions of natural killer cells. Nat Immunol. 2008; 9:503–510. [PubMed: 18425107]

19. Hochweller K, Striegler J, Hammerling GJ, Garbi N. A novel CD11c.DTR transgenic mouse for depletion of dendritic cells reveals their requirement for homeostatic proliferation of natural killer cells. European journal of immunology. 2008; 38:2776–2783. [PubMed: 18825750]

20. Koka R, Burkett P, Chien M, Chai S, Boone DL, Ma A. Cutting edge: murine dendritic cells require IL-15R alpha to prime NK cells. Journal of immunology. 2004; 173:3594–3598.

21. Lucas M, Schachterle W, Oberle K, Aichele P, Diefenbach A. Dendritic cells prime natural killer cells by trans-presenting interleukin 15. Immunity. 2007; 26:503–517. [PubMed: 17398124]

22. Schleicher U, Liese J, Knippertz I, Kurzmann C, Hesse A, Heit A, Fischer JA, Weiss S, Kalinke U, Kunz S, Bogdan C. NK cell activation in visceral leishmaniasis requires TLR9, myeloid DCs, and IL-12, but is independent of plasmacytoid DCs. The Journal of experimental medicine. 2007; 204:893–906. [PubMed: 17389237]

23. Ferlazzo G, Tsang ML, Moretta L, Melioli G, Steinman RM, Munz C. Human dendritic cells activate resting natural killer (NK) cells and are recognized via the NKp30 receptor by activated NK cells. The Journal of experimental medicine. 2002; 195:343–351. [PubMed: 11828009]
24. Bryceson YT, March ME, Ljunggren HG, Long EO. Activation, coactivation, and costimulation of resting human natural killer cells. Immunological reviews. 2006; 214:73–91. [PubMed: 17100877]
25. Karre K. Natural killer cell recognition of missing self. Nat Immunol. 2008; 9:477–480. [PubMed: 18425103]
26. Long EO. Negative signaling by inhibitory receptors: the NK cell paradigm. Immunological reviews. 2008; 224:70–84. [PubMed: 18759921]
27. Burshtyn DN, Scharenberg AM, Wagtmann N, Rajagopalan S, Berrada K, Yi T, Kinet JP, Long EO. Recruitment of tyrosine phosphatase HCP by the killer cell inhibitor receptor. Immunity. 1996; 4:77–85. [PubMed: 8574854]
28. Peterson ME, Long EO. Inhibitory receptor signaling via tyrosine phosphorylation of the adaptor Crk. Immunity. 2008; 29:578–588. [PubMed: 18835194]
29. Liu D, Peterson ME, Long EO. The adaptor protein Crk controls activation and inhibition of natural killer cells. Immunity. 2012; 36:600–611. [PubMed: 22464172]
30. Castillo EF, Schluns KS. Regulating the immune system via IL-15 transpresentation. Cytokine. 2012; 59:479–490. [PubMed: 22795955]
31. Sato N, Patel HJ, Waldmann TA, Tagaya Y. The IL-15/IL-15Ralpha on cell surfaces enables sustained IL-15 activity and contributes to the long survival of CD8 memory T cells. Proceedings of the National Academy of Sciences of the United States of America. 2007; 104:588–593. [PubMed: 17202253]
32. Robertson MJ, Cochran KJ, Cameron C, Le JM, Tantravahi R, Ritz J. Characterization of a cell line, NKL, derived from an aggressive human natural killer cell leukemia. Experimental hematology. 1996; 24:406–415. [PubMed: 8599969]
33. Shimizu Y, DeMars R. Production of human cells expressing individual transferred HLA-A,-B,-C genes using an HLA-A,-B,-C null human cell line. Journal of immunology. 1989; 142:3320–3328.
34. Cohen GB, Gandhi RT, Davis DM, Mandelboim O, Chen BK, Strominger JL, Baltimore D. The selective downregulation of class I major histocompatibility complex proteins by HIV-1 protects HIV-infected cells from NK cells. Immunity. 1999; 10:661–671. [PubMed: 10403641]
35. Stebbins CC, Watzl C, Billadeau DD, Leibson PJ, Burshtyn DN, Long EO. Vav1 dephosphorylation by the tyrosine phosphatase SHP-1 as a mechanism for inhibition of cellular cytotoxicity. Molecular and cellular biology. 2003; 23:6291–6299. [PubMed: 12917349]
36. Lee N, Llano M, Carretero M, Ishitani A, Navarro F, Lopez-Botet M, Geraghty DE. HLA-E is a major ligand for the natural killer inhibitory receptor CD94/NKG2A. Proceedings of the National Academy of Sciences of the United States of America. 1998; 95:5199–5204. [PubMed: 9560253]
37. Burshtyn DN, Shin J, Stebbins C, Long EO. Adhesion to target cells is disrupted by the killer cell inhibitory receptor. Current biology: CB. 2000; 10:777–780. [PubMed: 10898979]
38. Wagtmann N, Rajagopalan S, Winter CC, Peruzzi M, Long EO. Killer cell inhibitory receptors specific for HLA-C and HLA-B identified by direct binding and by functional transfer. Immunity. 1995; 3:801–809. [PubMed: 8777725]
39. Biassoni R, Cantoni C, Falco M, Verdiani S, Bottino C, Vitale M, Conte R, Poggi A, Moretta A, Moretta L. The human leukocyte antigen (HLA)-C-specific “activatory” or “inhibitory” natural killer cell receptors display highly homologous extracellular domains but differ in their transmembrane and intracytoplasmic portions. The Journal of experimental medicine. 1996; 183:645–650. [PubMed: 8627176]
40. Wagtmann N, Biassoni R, Cantoni C, Verdiani S, Malnati MS, Vitale M, Bottino C, Moretta L, Moretta A, Long EO. Molecular clones of the p58 NK cell receptor reveal immunoglobulin-related molecules with diversity in both the extra- and intracellular domains. Immunity. 1995; 2:439–449. [PubMed: 7749980]
41. Saleiro D, Platanias LC. Intersection of mTOR and STAT signaling in immunity. Trends in immunology. 2015; 36:21–29. [PubMed: 25592035]

42. Tripathi P, Kurtulus S, Wojciechowski S, Sholl A, Hoebe K, Morris SC, Finkelman FD, Grimes HL, Hildeman DA. STAT5 is critical to maintain effector CD8+ T cell responses. Journal of immunology. 2010; 185:2116–2124.
43. Hand TW, Cui W, Jung YW, Sefik E, Joshi NS, Chandele A, Liu Y, Kaech SM. Differential effects of STAT5 and PI3K/AKT signaling on effector and memory CD8 T-cell survival. Proceedings of the National Academy of Sciences of the United States of America. 2010; 107:16601–16606. [PubMed: 20823247]
44. Brilot F, Strowig T, Roberts SM, Arrey F, Munz C. NK cell survival mediated through the regulatory synapse with human DCs requires IL-15Ralpha. The Journal of clinical investigation. 2007; 117:3316–3329. [PubMed: 17948125]
45. Long EO, Kim HS, Liu D, Peterson ME, Rajagopalan S. Controlling natural killer cell responses: integration of signals for activation and inhibition. Annual review of immunology. 2013; 31:227–258.
46. Barreira da Silva R, Graf C, Munz C. Cytoskeletal stabilization of inhibitory interactions in immunologic synapses of mature human dendritic cells with natural killer cells. Blood. 2011; 118:6487–6498. [PubMed: 21917751]
47. Liu D, Meckel T, Long EO. Distinct role of rab27a in granule movement at the plasma membrane and in the cytosol of NK cells. PloS one. 2010; 5:e12870. [PubMed: 20877725]
48. Schleinitz N, March ME, Long EO. Recruitment of activation receptors at inhibitory NK cell immune synapses. PloS one. 2008; 3:e3278. [PubMed: 18818767]
49. Imada K, Leonard WJ. The Jak-STAT pathway. Molecular immunology. 2000; 37:1–11. [PubMed: 10781830]
50. Ruvinsky I, Meyuhas O. Ribosomal protein S6 phosphorylation: from protein synthesis to cell size. Trends Biochem Sci. 2006; 31:342–348. [PubMed: 16679021]
51. Marcais A, Cherfils-Vicini J, Viant C, Degouve S, Viel S, Fenis A, Rabilloud J, Mayol K, Tavares A, Bienvenu J, Gangloff YG, Gilson E, Vivier E, Walzer T. The metabolic checkpoint kinase mTOR is essential for IL-15 signaling during the development and activation of NK cells. Nature immunology. 2014; 15:749–757. [PubMed: 24973821]
52. Klingmuller U, Lorenz U, Cantley LC, Neel BG, Lodish HF. Specific recruitment of SH-PTP1 to the erythropoietin receptor causes inactivation of JAK2 and termination of proliferative signals. Cell. 1995; 80:729–738. [PubMed: 7889566]
53. Elpek KG, Rubinstein MP, Bellemare-Pelletier A, Goldrath AW, Turley SJ. Mature natural killer cells with phenotypic and functional alterations accumulate upon sustained stimulation with IL-15/IL-15Ralpha complexes. Proceedings of the National Academy of Sciences of the United States of America. 2010; 107:21647–21652. [PubMed: 21098276]

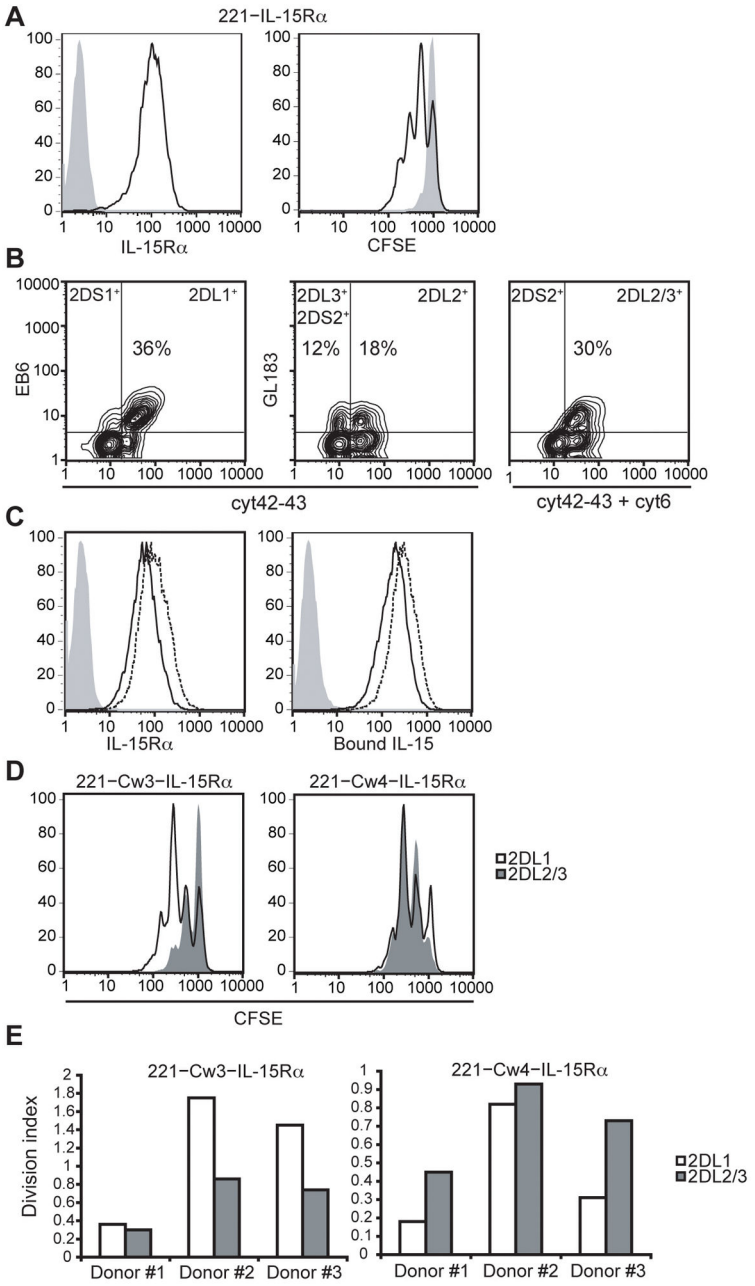

FIGURE 1.

NK cell proliferation induced by IL-15 transpresentation is reduced by simultaneous engagement of inhibitory KIR. (**A**) Expression of IL-15Rα on transduced 721.221 cells (left panel). Shaded histogram represents staining with an isotype control antibody. Right panel, CFSE dilution in NK cells mixed for 5 days with 221–IL-15Rα cells (shaded histogram) or 221–IL-15Rα cells that had been preloaded with IL-15 (black line). (**B**) Primary, resting NK cells were stained with mAb EB6 specific for KIR2DL1 and KIR2DS1, and with mAb GL183, specific for KIR2DL2, KIR2DL3 and KIR2DS2. After fixation and permeabilization cells were stained with rabbit polyclonal antiserum cyt42-43, specific for

the C-terminal end of the cytoplasmic tail of KIR2DL1 and KIR2DL2, and cyt42-43 in combination with cyt6, which reacts with the C-terminal end of the tail of KIR2DL3. (**C**) Left panel, expression of IL-15Rα on transfected 221–Cw3–IL-15Rα cells (dotted line) and 221–Cw4–IL-15Rα cells (solid line) that had been preloaded with IL-15. The shaded histogram represents staining with an isotype control antibody. Right panel, IL-15 bound to 221–Cw3–IL-15Rα (dotted line) and 221–Cw4–IL-15Rα (solid line) after preloading. The shaded histogram represents staining of 221 cells not loaded with IL-15. (**D**) NK cells 5 days after CFSE labeling and mixing with 221–Cw3–IL-15Rα (left panel) or 221–Cw4–IL-15Rα (right panel) cells that had been pre-loaded with IL-15. The black line represents a gate of NK cells positive for KIR2DL1 and negative for KIR2DL2/3, NKG2A and NKG2C. The shaded histogram represents a gate of NK cells positive for KIR2DL2/3 and negative for KIR2DL1, NKG2A and NKG2C. (**E**) Proliferation analysis of NK cells from three different donors, performed and gated as in **D**. CFSE dilution measured by flow cytomety was analyzed with the FlowJo proliferation platform, and data is presented as division index.

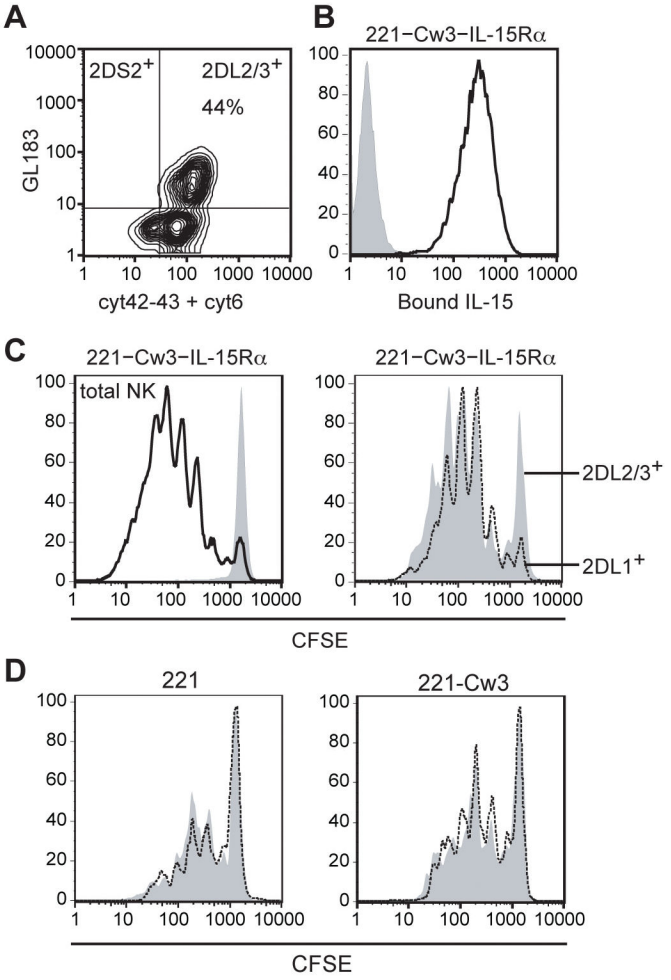

FIGURE 2.

KIR inhibits NK cell proliferation induced by transpresented but not soluble IL-15. (**A**) Identification of a donor that lacks expression of KIR2DS2. Primary, resting NK cells were stained with mAb GL183 specific for KIR2DL2, KIR2DL3 and KIR2DS2, and after fixation and permeabilization cells were stained with rabbit polyclonal antiserum cyt42-43 specific for the cytoplasmic tails of KIR2DL1 and KIR2DL2, and with cyt6, which reacts with the cytoplasmic tail of KIR2DL3. (**B**) IL-15 bound to 221–Cw3–IL-15Rα cells was detected with an antibody to IL-15. The shaded histogram represents cells not loaded with IL-15. (**C**) CFSE dilution in NK cells 5 days after CFSE labeling and mixing with 221–Cw3–IL-15Rα cells that had been either preloaded (solid line) or not (shaded) with IL-15 (left panel). In the same sample, CFSE dilution was monitored in cells gated for KIR2DL1$^+$ and negative for KIR2DL2/3, NKG2A and NKG2C (dotted line) versus cells gated for KIR2DL2/3$^+$ and negative for KIR2DL1, NKG2A and NKG2C (shaded). (**D**) CFSE dilution in NK cells 5 days after mixing with untransfected 221 cells (left panel) or 221–Cw3 cells (right panel) in the presence of 50 nM soluble IL-15. Cells were gated for KIR2DL1$^+$ (dotted line) and KIR2DL2/3$^+$ (shaded) as in C.

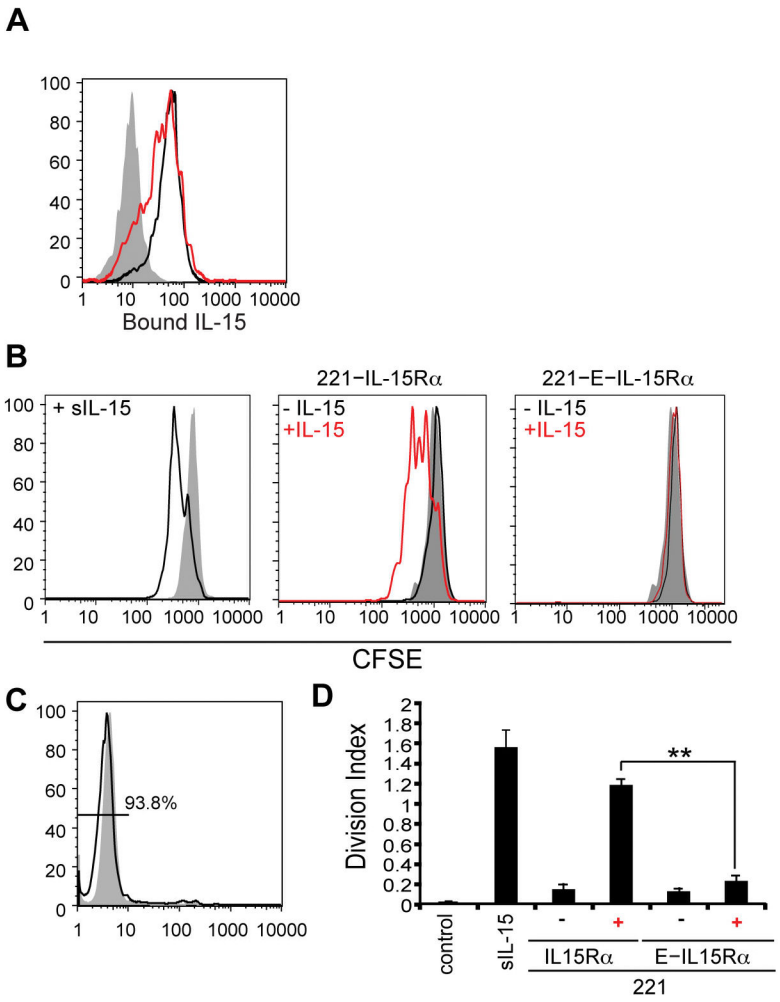

FIGURE 3.

Proliferation of NKL cells induced by IL-15 transpresentation is inhibited by simultaneous engagement of CD94-NKG2A. (**A**) Staining of IL-15 on 221–IL-15Rα cells (black line) and 221–E–IL-15Rα cells (red line) after preloading with IL-15. The shaded histogram represents 221–E–IL-15Rα cells not loaded with IL-15. (**B**) Rested NKL cells were labeled with CFSE and incubated for 3 days with 50 nM soluble IL-15 (sIL-15) (left panel) or 3 days with 221–IL-15Rα or 221–E–IL-15Rα cells, as indicated, that had been preloaded (red line) or not (black line) with IL-15. Shaded histograms represent NKL cells incubated with 221 cells not loaded with IL-15. A representative experiment out of three independent experiments performed is shown here. (**C**) PI staining of NKL cells 3 days after mixing with IL-15-preloaded 221–IL-15Rα cells (shaded) or 221–E–IL-15Rα cells (dark line). (**D**) Division Index representation, as calculated by FlowJo. Transfected 221 cells that were pre-loaded with IL-15 are indicated (red +). Histograms represent mean and standard deviation of three independent proliferation experiments. **p< 0.01

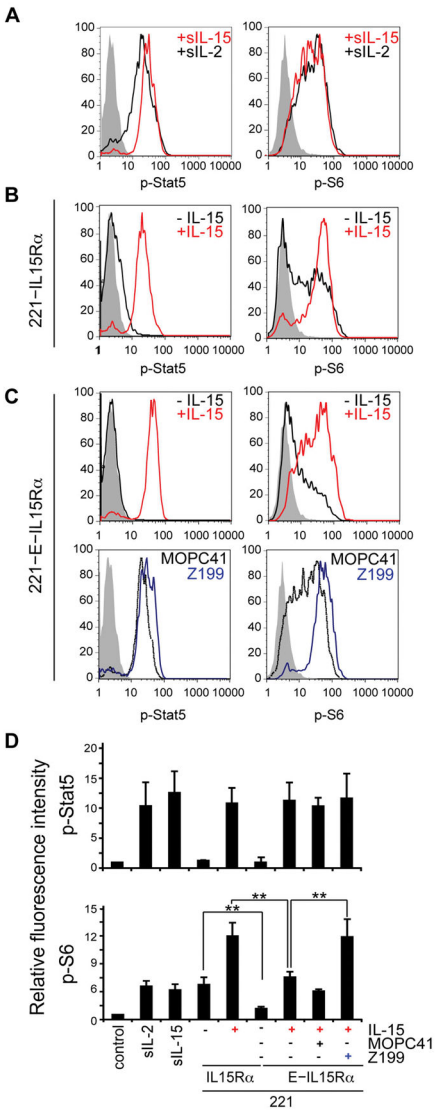

FIGURE 4.

Phosphorylation of S6 but not Stat5 is inhibited by CD94-NKG2A. (**A**) Phosphorylation of Stat5 (left panels) and S6 (right panels) in NKL cells detected by intracellular flow cytometry after addition of 50 nM soluble IL-15 (sIL-15, red) or 100 U/ml soluble IL-2 (sIL-2, black). (**B**) Phosphorylation of Stat5 and S6 in NKL cells 1 hour after mixing with 221–IL-15Rα cells pre-loaded (red line) or not (black line) with IL-15. (**C**) Phosphorylation of Stat5 and S6 in NKL cells 1 hour after mixing with 221–E–IL-15Rα cells pre-loaded (red line) or not (black line) with IL-15 (top panels). Blocking anti-NKG2A antibody Z199 was added at 1 μg/ml (blue) to NKL cells 30 min prior to the incubation with 221–E–IL-15Rα cells (lower panels). Isotype control MOPC41 (mIgG2b) was added to the cells at the same concentration (dotted). In panels A, B, C, shaded histograms represent isotype control antibody staining. (**D**) Quantitation of Stat5 and S6 phosphorylation in three independent experiments. Transfected 221 cells that were pre-loaded with IL-15 are indicated (red +).

MOPC41 and Z199 Abs were added where indicated (+). Data are represented as relative fluorescence intensity with the standard deviation in each case. **p< 0.01

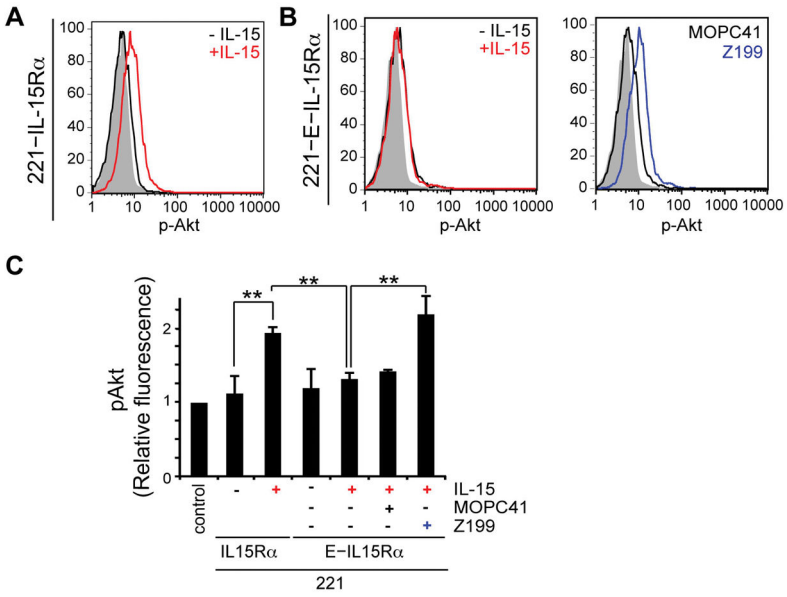

FIGURE 5.

Phosphorylation of Akt induced by IL-15 transpresentation is inhibited by CD94-NKG2A. (**A**) Phosphorylation of Akt (S473) in NKL cells detected by intracellular flow cytometry 30 min after mixing with 221–IL-15Rα pre-loaded (red line) or not (black line) with IL-15. (**B**) Phosphorylation of Akt 30 min after mixing with 221–E–IL-15Rα cells pre-loaded (red line) or not (black line) with IL-15 (left panels). Blocking anti-NKG2A antibody Z199 was added at 1 μg/ml (blue) to NKL cells 30 min prior to the incubation with 221–E–IL-15Rα cells (right panel). Isotype control MOPC41 (mIgG2b) was added to the cells at the same concentration (black). In panels A and B shaded histograms represent isotype control antibody staining. (**C**) Quantitation of Akt phosphorylation in three independent experiments. Transfected 221 cells that were preloaded with IL-15 are indicated (red +). MOPC41 and Z199 Abs were added where indicated (+). Data are represented as relative fluorescence intensity with the standard deviation in each case. **p< 0.01

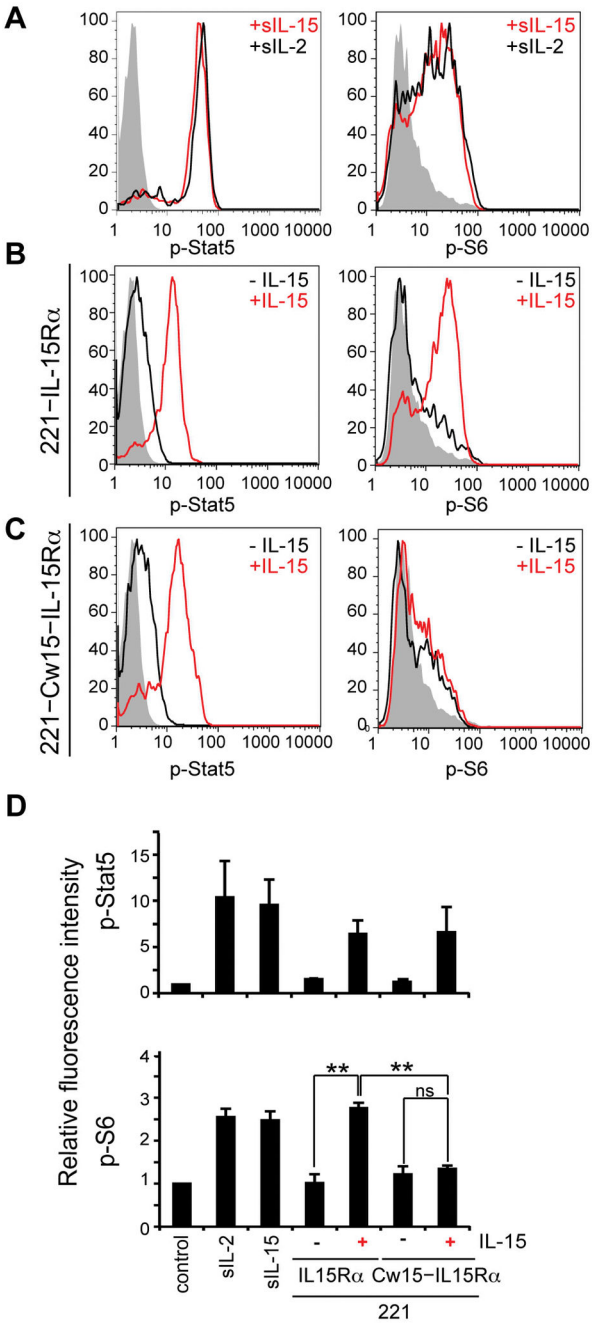

FIGURE 6.

Phosphorylation of S6, but not Stat5, induced by IL-15 transpresentation is inhibited by KIR2DL1. (**A**) Phosphorylation of Stat5 (left panels) and S6 (right panels) in NKL-2DL1 cells detected by intracellular flow cytometry after addition of 50 nM soluble IL-15 (sIL-15, red) or 100 U/ml soluble IL-2 (sIL-2, black). (**B**) Phosphorylation of Stat5 and S6 in NKL-2DL1 cells 1 hour after mixing with 221–IL-15Rα pre-loaded (red line) or not (black line) with IL-15. (**C**) Phosphorylation of Stat5 and S6 in NKL-2DL1 cells 1 hour after mixing with 221–Cw15–IL-15Rα cells pre-loaded (red line) or not (black line) with IL-15.

In A, B, C, shaded histograms represent staining in untreated NKL-2DL1. (**D**) Quantitation of Stat5 and S6 phosphorylation in three independent experiments. Transfected 221 cells that were pre-loaded with IL-15 are indicated (red +). Data are represented as relative fluorescence intensity with the standard deviation in each case. **p< 0.01

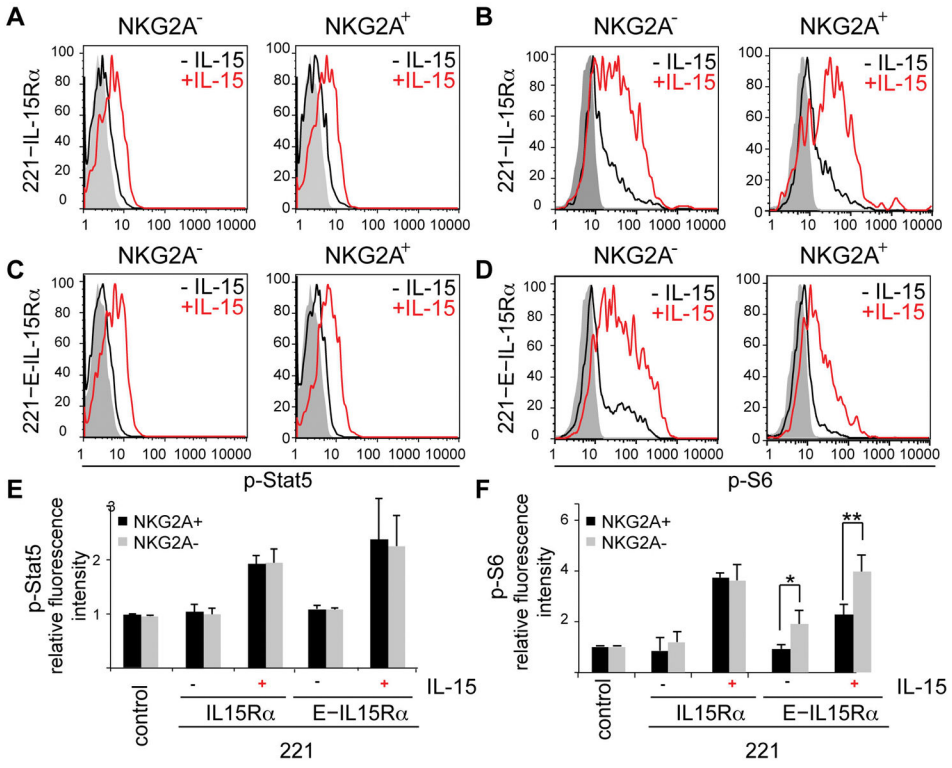

FIGURE 7.

Phosphorylation of S6 but not Stat5 induced by IL-15 transpresentation is inhibited by CD94-NKG2A in primary human NK cells. NKG2C-depleted $CD56^+$ cells were gated for NKG2A-negative cells (left panel) and $NKG2A^+$ cells (right panels), as indicated. (**A**) Phosphorylation of Stat5 in primary NK cells detected by intracellular flow cytometry 1 hour after mixing with 221–IL-15Rα pre-loaded (red line) or not (black line) with IL-15. (**B**) Phosphorylation of S6 in primary NK cells detected by intracellular flow cytometry 1 hour after mixing with 221–IL-15Rα cells pre-loaded (red line) or not (black line) with IL-15. In A, B, shaded histograms represent staining in untreated NK cells. (**C**) Phosphorylation of Stat5 in primary NK cells detected 1 hour after mixing with 221–E–IL-15Rα pre-loaded (red line) or not (black line) with IL-15. (**D**) Phosphorylation of S6 in primary NK cells detected 1 hour after mixing with 221–E–IL-15Rα cells preloaded (red line) or not (black line) with IL-15. In C, D, shaded histograms represent staining in untreated NK cells. (**E**) Quantitation of Stat5 phosphorylation in three independent experiments shown as relative to the control (untreated NK cells). Transfected 221 cells that were pre-loaded with IL-15 are indicated (red +). $NKG2A^+$ cells are represented by black bars. NKG2A-negative cells are represented by shaded bars. (**F**) Quantitation of S6 phosphorylation in three independent experiments shown as relative to the control (untreated NK cells). Transfected 221 cells that had been preloaded with IL-15 are indicated by a red + symbol. $NKG2A^+$ cells are represented by black bars. NKG2A-negative cells are represented by shaded bars. **p< 0.01

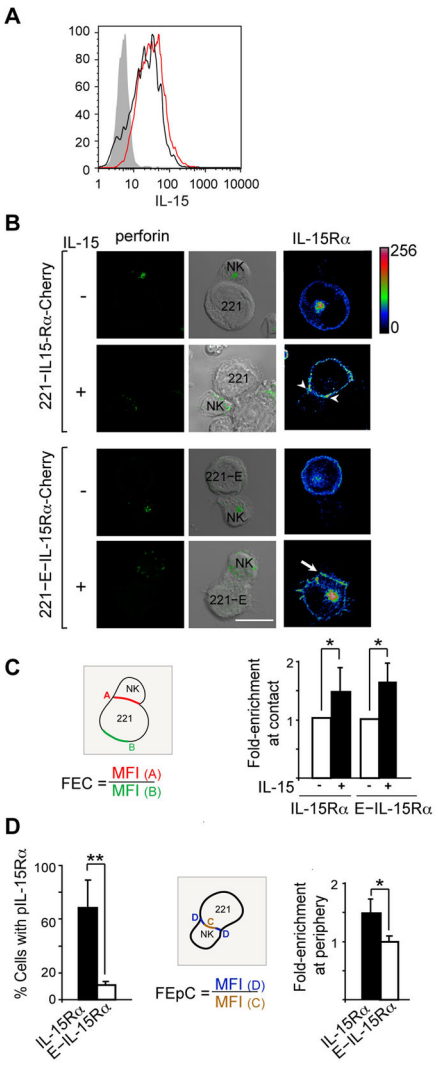

FIGURE 8.

IL-15Rα is uniformly distributed at inhibitory NK–target cell synapses. (**A**) IL-15 bound to IL-15Rα fused to mCherry and expressed on 221 (black) and 221–E (red) cells, after preloading with IL-15. The shaded histogram represents isotype control antibody staining. (**B**) 221–IL-15Rα-Cherry and 221–E–IL-15Rα-Cherry cells were preloaded or not with IL-15, as indicated, and mixed with NKL cells for 15 minutes, fixed, permeabilized and stained with an antibody to perforin (left). Overlay of perforin staining onto DIC images shows reduced perforin polarization toward 221–E cells. IL-15Rα-mCherry intensity is shown in a false color scale on the right. Arrowheads indicate accumulation of IL-15Rα at the contact of 221–IL-15Rα cells with NKL cells. The arrow indicates accumulation of IL-15Rα at the contact of 221–E–IL-15Rα cells with NKL cells. Scale bar, 5 μm. (**C**) The fluorescence enrichment of IL-15Rα at the contact (FEC) was quantitated by ImageJ and expressed as the mean fluorescence intensity at the contact area (MFI_A) divided by the mean fluorescence intensity at the opposite pole of the cell (MFI_B). The histograms show the FEC for the indicated cells either pre-loaded (black bars) or not (open bars) with IL-15. Data are

shown as the mean and standard deviation. (**D**) Quantitation of the number of cells with IL-15Rα accumulated at the periphery of the contact. The data is expressed as percentage of cells in relation to the total number of synapses quantified in each case. To quantitate the fluorescence enrichment of IL-15Rα at the periphery of the contact (FEpC), the mean fluorescence intensity at the distal part of the contact (MFI_D) was divided by the mean fluorescence intensity at the center of the contact (MFI_C). The histogram on the right shows the FEpC expressed as fold-enrichment of the fluorescence signal at the contact in each case. Data are shown as the mean and standard deviation (n=20 cells in total from three independent experiments). * $p < 0.05$